JOURNAL OF MATERIALS SCIENCE 27 (1992) 6187–6192

Chemical vapour deposited *in-situ* composites in the system Ti–Si–C

M. MALINE, R. HILLEL
Laboratory of IMP-CNRS, University of Perpignan, 66860 Perpignan Cedex, France
R. BERJOAN
Laboratory of IMP-CNRS, B.P.5-Odeillo, 66120 Font-Romeu, France

Chemical vapour deposited (CVD) SiC–ceramic composites were produced by adding $TiCl_4$ to the SiH_2Cl_2–C_4H_{10}–H_2 system previously used to prepare CVD β-SiC. Experiments performed in a classical cold-wall reactor on a graphite substrate heated by Joule effect, were carried out at a constant hydrogen gas flow rate of $30\ l\ h^{-1}$, under atmospheric pressure and at a deposition temperature ranging from 1123–1373 K. Silicon, titanium and carbon elemental compositions were determined by electron probe microanalysis-wavelength dispersive spectrometry. Phase identifications were mainly performed by Auger electron spectroscopy and X-ray diffraction and additionally by Raman spectroscopy. Three- and two-phased materials were obtained: SiC–TiC–C, SiC–TiC and SiC–$TiSi_2$ with ratios $4 < SiC/TiC < 19$ and $1.5 < SiC/TiSi_2 < 11$. Temperature governed the dominance of the dispersed phases: lower for $TiSi_2$ and higher for TiC than TiC + C. At 1373 K, co-deposits were strongly textured, the β-SiC [2 2 0] preferred orientation getting weaker as the deposition temperature decreased. Apparent crystallite size along the ⟨2 2 0⟩ direction decreased with temperature from about 15 nm to 10 nm. The deposition rate was almost independent of time and decreased with temperature from about $800\ \mu m\ h^{-1}$ to $60\ \mu m\ h^{-1}$. Arrhenius plots showed linear relationships with temperature and slope breaks at 1123 K, the temperature corresponding to the change of the dispersed phases in the SiC matrix.

1. Introduction

Chemical vapour deposited (CVD) SiC is an attractive material because of its outstanding properties such as high hardness, high-temperature corrosion resistance, wear resistance, and thermal-shock resistance [1, 2]. For instance, it is the matrix most commonly used to densify porous materials, specially fibre preforms [3]. It is also a promising resistant coating for protecting tools and advanced structural forms [4, 5]. Unfortunately, as well as other ceramics, the brittleness of the CVD SiC limits its use under high contact and structural stress. In agreement with the fact that an increase in fracture toughness can be obtained by the incorporation of a second phase in ceramic bodies, improved CVD SiC has already been obtained at ~ 1673 K by co-deposition of SiC as a major phase with fine particles of $TiSi_2$ uniformly dispersed in it [6]. SiC–TiC co-deposits were also prepared between 1473 and 1673 K [7] and thoroughly studied in our laboratory by Touanen [8, 9]. This recent work confirmed that CVD is an effective method for providing multiphased deposition near to equilibrium conditions and allowing control of the amount and size of the dispersed phases.

In the research reported here, the originality lies in the fact that the co-deposition temperatures were selected in a domain mostly used in chemical vapour infiltration and CVD surface treatments, i.e. 1373–1123 K. In this range, SiC–ceramic nanocomposites with dispersed TiC or $TiSi_2$, depending on temperature, have been produced with controlled composition.

2. Experimental procedure

Deposits were prepared by conventional thermal CVD, under atmospheric pressure. The experimental device was a typical cold-wall reactor. The reactor chamber consisted of a vertical silica tube (diameter = 5.0 cm, $L = 20$ cm). It should be mentioned that the reactants were flowing from the bottom upwards in order to minimize the thermal effect. The CVD was performed on mechanically polished polycrystalline graphite substrates (thickness = 1 mm) (le Carbone-Lorraine 1116 PT) heated by transmitting an electric current, the substrate shape being designed in order to obtain a uniformly heated zone of $25 \times 5\ mm^2$. Liquid $TiCl_4$, gaseous C_4H_{10} and SiH_2Cl_2 in hydrogen gas were used as reactant sources. This gas mixture was recently chosen in our laboratory from thermodynamic criteria [10, 11]. The hydrogen gas flow rate was kept constant at $30\ l\ h^{-1}$ and two precursor compositions were investigated. SiC samples, as reference matrix, and $TiSi_2$ were also CVD prepared using

0022–2461 © 1992 Chapman & Hall

TABLE I Experimental deposition conditions (D_{H_2} = 30 l h^{-1}, P = 1 atm, t = 0.5 h)

	Flow rate (l h^{-1} TPN)			Temperature (K)
	D_{TiCl_4}	$D_{SiH_2Cl_2}$	$D_{C_4H_{10}}$	
SiC		0.925	0.811	1373, 1273
$TiSi_2$	0.182	0.316		1123
Co-deposits:				
1st set of conditions	0.182	0.544	0.992	1373, 1323 1273, 1223
2nd set of conditions	0.182	0.925	0.811	1173, 1123

the same precursors. The deposition conditions are summarized in Table I.

3. Coating characterization techniques

Silicon, titanium and carbon elemental compositions were determined by electron probe microanalysis–wavelength dispersive spectrometry (EPMA–WDS Camebax equipped with ODPb wavelength dispersive spectrometer, I = 70–100 nA, V = 10 kV, standards = SiC, TiC). Phase identifications were mainly performed by Auger electron spectroscopy (AES, Riber SIA-200, I = 200–300 nA, E_p = 3–5 keV), and X-ray diffraction (XRD, Philips PW 1710, CoK_α = 0.179 02 nm, 40 kV) and additionally by Raman spectroscopy (Coderg, 514.5 nm radiation). XRD was used to identify texture and to evaluate crystallite size. The thickness of the deposits was measured on metallographic cross-sections.

4. Results and discussion

4.1. Phase identification and molar compositions

Depending on the initial gas mixture composition and on the temperature deposition, three types of sample were produced: three-phased SiC–TiC–C and two-phased SiC–TiC and SiC–$TiSi_2$. The evolution of their molar composition as a function of temperature (Fig. 1a and b) shows that temperature is a factor governing the dominance of the dispersed phases: a lower temperature for $TiSi_2$ and a higher temperature for TiC than TiC + C. The higher the temperature, the larger was the amount of free carbon. Although the number of experiments was insufficient to discuss the whole effect of the input gas phase, it was obvious that an increase of C_4H_{10} produced a greater free carbon amount and consequently less TiC. Taking into account all the samples, it is worth noting that when free carbon was absent, two-phased coatings were produced with $4 < SiC/TiC < 19$ and $1.5 < SiC/TiSi_2 < 11$. After the phases SiC and TiC or $TiSi_2$ were identified, molar compositions were calculated from EPMA–WDS determinations of the silicon, titanium and carbon atomic percentages. When silicon and titanium were present as carbide phases, as was the case for materials deposited at high temperature, the atomic ratio Si/C was smaller than 1 and the amount of free carbon was easily deduced. On the other hand,

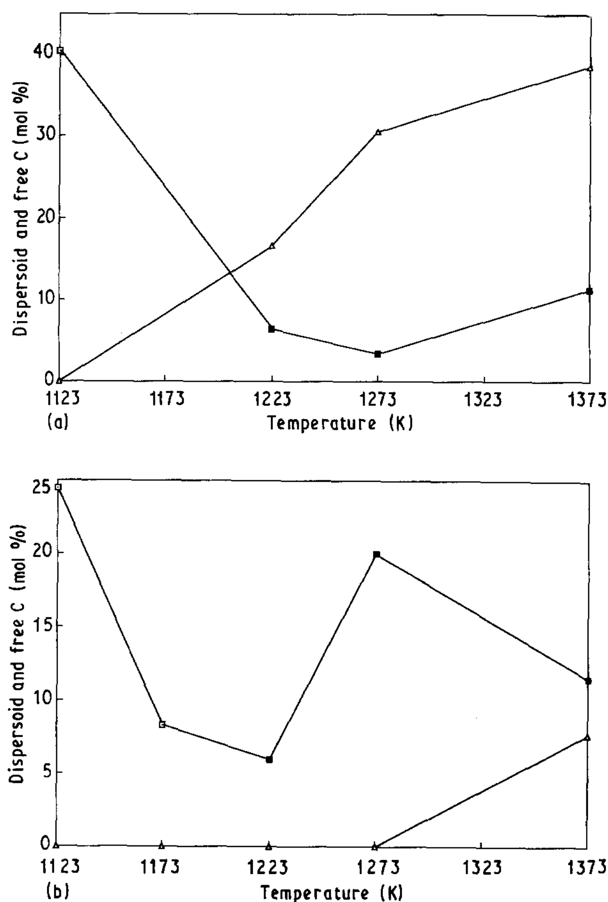

Figure 1 Dispersoïd and free-carbon molal percentages versus the deposition temperature. (a) First set of conditions: initial gas mixture composition $x_{Ti} = 2.81 \times 10^{-3}$, $x_{Si} = 8.41 \times 10^{-3}$, $x_C = 61.33 \times 10^{-3}$, $x_H = 0.927$. (b) Second set of conditions: initial gas mixture composition $x_{Ti} = 2.83 \times 10^{-3}$, $x_{Si} = 14.37 \times 10^{-3}$, $x_C = 50.41 \times 10^{-3}$, $x_H = 0.932$. Dispersed phases: (□) $TiSi_2$, (■) TiC. (△) Free carbon.

when Si/C > 1 only SiC and $TiSi_2$ were co-deposited. SiC matrix and TiC or $TiSi_2$ as dipersoids were identified using Auger spectroscopy. AES spectra were recorded in the direct $N(E)$ mode. Before spectrum scanning, the sample surfaces were cleaned and etched by argon ion sputtering using an ion gun producing 3 keV Ar^+ ions. Fig. 2 shows low-energy range Auger $E.N(E)$ spectra (50–540 eV; operating conditions: E_p = 3 keV, I = 200 mA, ΔE = 1 eV) of three chosen samples of the following molal compositions (calculated from EPMA–WDS determinations): Sample 1, 59.5 SiC–40.5 $TiSi_2$; Sample 2, 80.0 SiC–20.0 TiC; Sample 3, 50.4 SiC–11.0 TiC–38.6 C (mol %). These spectra were compared with those of reference samples CVD TiC, CVD β-SiC and monocrystalline $TiSi_2$. The Si LVV peak position for $TiSi_2$ is 89.5 eV, very close to 89 eV for pure silicon [12], whereas for SiC this valence–valence transition is located at 87 eV. The same values are found in Auger spectra for Samples 2 and 3, whereas 88 eV is the peak position in the case of Sample 1. Moreover, the Si LVV peak shapes for SiC, Samples 2 and 3 are broadened in comparison with those for Sample 1 and especially $TiSi_2$. In the C KVV transition, we note that the peak position for SiC is shifted to lower energy (267 eV) than for the TiC (269 eV) value found for Samples 2 and 3. On the other hand, Sample 1 shows a C KVV peak whose position

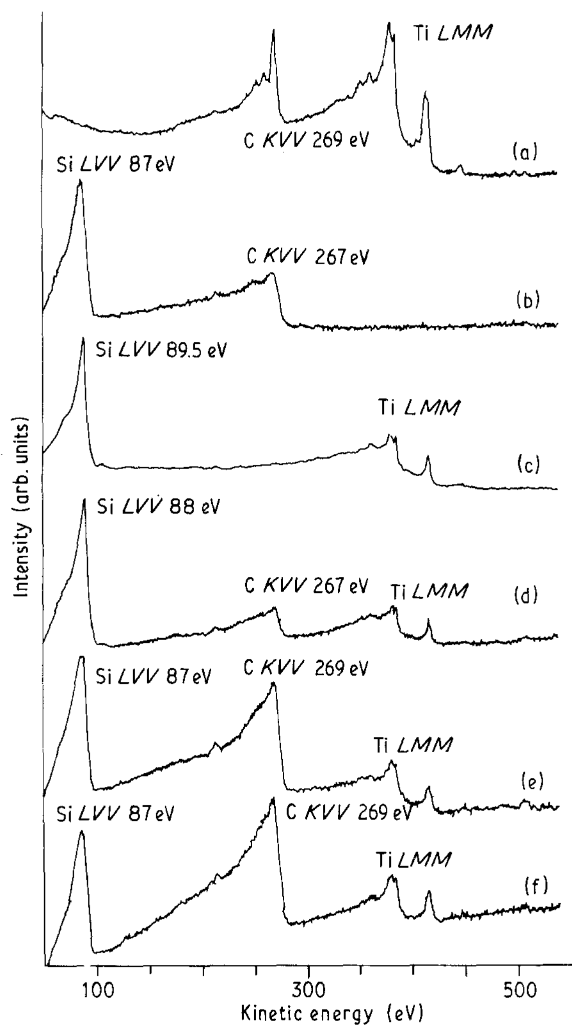

Figure 2 Low-energy range AES spectra (I = 200 nA, E_p = 3 keV, ΔE = 1 eV). (a) CVD TiC, (b) CVD SiC, (c) monocrystalline $TiSi_2$, (d) Sample 1, codeposit produced at 1123 K under first set of conditions = 59.5 SiC–40.5 $TiSi_2$ mol %. (e) Sample 2, codeposit produced at 1273 K under second set of conditions = 80.0 SiC–20.0 TiC mol %. (f) Sample 3, codeposit produced at 1373 K under first set of conditions = 50.4 SiC–11.0 TiC–38.6 C mol %.

is the same as for SiC with a very similar shape. These results are in agreement with the molar compositions previously attributed to the samples, and in addition with the features of Ti *LMM* Auger transitions.

Now let us examine the $N(E)$ L_3 M_{23} M_{23} and L_3 M_{23} M_{45} Auger transitions of titanium recorded in the range 350–430 eV (Fig. 3). For $TiSi_2$, this transition presents a clearly resolved double structure corresponding to ^{3}P and ^{1}D terms respectively at 386 and 381 eV, whereas for TiC a less-well resolved structure is found. Also, the $L_3M_{23}M_{23}$ transition for TiC is shifted to lower energies: ^{3}P at 384.5 eV and ^{1}D at 380 eV. The $L_3M_{23}M_{23}$ transition feature recorded for Sample 2 is similar to that for TiC and the structure observed for Sample 1 is similar to that for $TiSi_2$. On the other hand, the $L_3M_{23}M_{45}$ transition (about 415 eV) for Sample 1 is similar to that for $TiSi_2$. For TiC and for Sample 2, this last transition is broadened. The width at half-height changes from about 4 eV for $TiSi_2$ and Sample 1 to about 6 eV for TiC and Sample 2. A careful examination of the Si $KL_{23}L_{23}$ core–core Auger transitions (Fig. 4) can also provide information concerning the atoms which

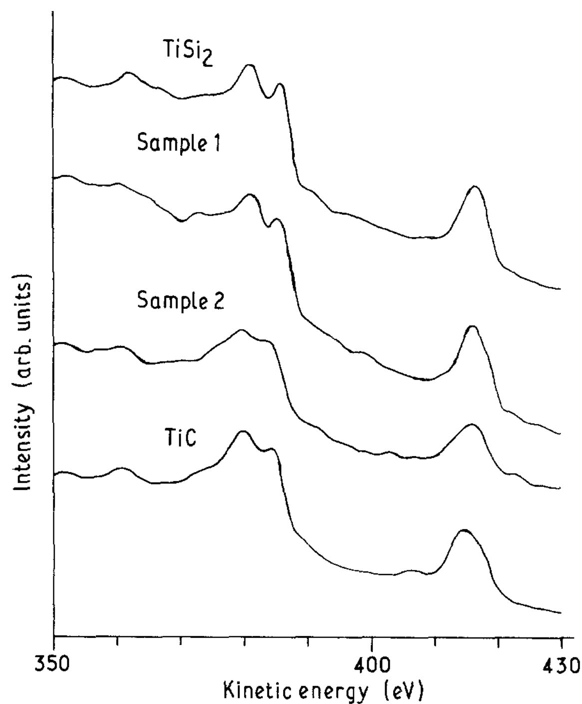

Figure 3 Ti LMM Auger spectra. Operating conditions I = 200 nA, E_p = 3 keV, ΔE = 1 eV.

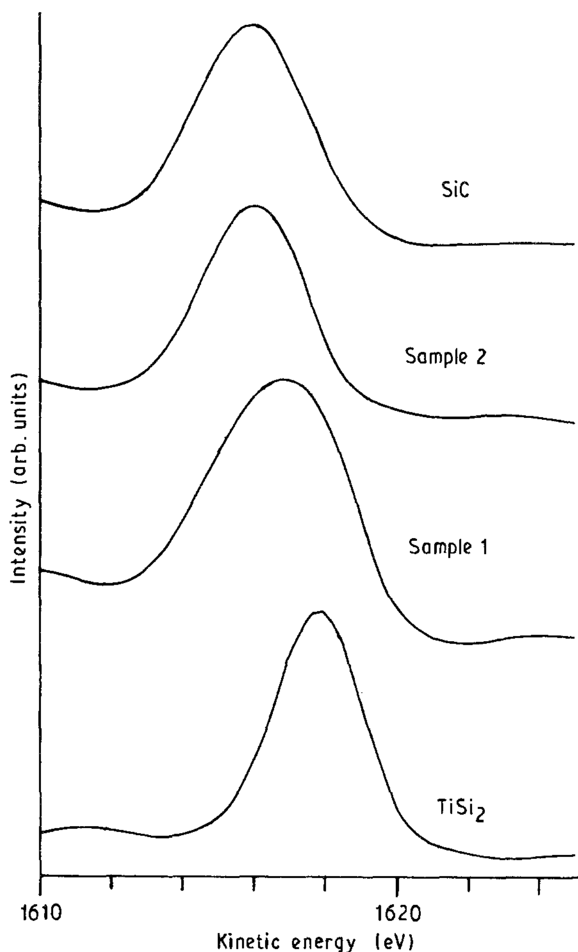

Figure 4 Si KLL Auger spectra. Operating conditions I = 300 nA, E_p = 5 keV, ΔE = 2 eV.

are bonded to silicon. The peak shape for Sample 2 is identical to that for SiC and its position is located at the same energy (1616 eV) as for SiC. We can conclude that in this sample, silicon is only bonded to carbon,

whereas for Sample 1, we note a very broad Si $KL_{23}L_{23}$ transition which occurs between those for $TiSi_2$ (1618 eV) and SiC (1616 eV). This broadened peak shape suggests the presence of both Si–C and Si–Ti bonds.

XRD was inefficient in identifying SiC, TiC and free carbon in materials prepared at high temperature (Si/C < 1). On the one hand, carbon was amorphous as detected by Raman spectroscopy. Indeed, while in "perfect" graphite the only allowed line is at 1580 cm^{-1} [13, 14], co-deposits containing free carbon exhibited the well-known additional disorder-induced line at 1360 cm^{-1} [14, 15] (Fig. 5). The ratio of their intensities I_{1360}/I_{1580} considered as a measure of disorder, was about 0.98 close to 1.2, the higher value corresponding to some amorphous carbon [13]. On the other hand, with SiC–TiC co-deposits, both the carbides were cubic, their cell parameters being very close (β-SiC, $a = 0.4358$ nm, JCPDS no. 1–1119; TiC, $a = 0.4328$ nm, JCPDS no. 6–0614) and so the X-ray diffraction lines were superimposed (Fig. 6, Spectra 2 and 3). On the contrary, in materials co-deposited at low temperature (Si/C > 1), SiC and $TiSi_2$ were unambiguously identified by XRD. The presence of $TiSi_2$ was supported by comparing its X-ray diffraction pattern with that of a $TiSi_2$ coating CVD prepared at 1123 K (Fig. 6, Spectra 4 and 5) and whose X-ray reflections (especially the four more intense lines: $d_{311} = 0.230$, $d_{040} = 0.214$, $d_{022} = 0.209$ and $d_{331} = 0.183$ nm) fitted those given in the JCPDS (no. 35–785: orthorhombic cell). The X-ray diffraction lines corresponding to β-SiC, $d_{111} = 0.251$, $d_{200} = 0.217$, $d_{220} = 0.154$ and $d_{311} = 0.131$ nm (Fig. 6, Spectrum 4) were assigned by comparison with those listed in the JCPDS.

4.2. Texture and crystallite size

With an SiC matrix in which TiC was dispersed, phase identification by XRD was all the more difficult because at high temperature the coatings were strongly textured. In fact, the X-ray diffraction patterns of co-deposits obtained above 1273 K exhibited only the

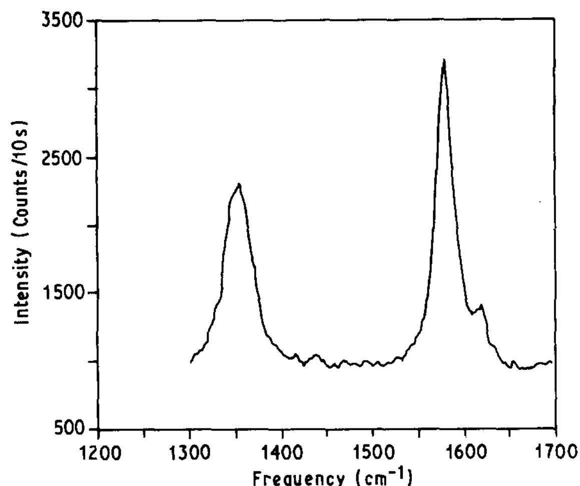

Figure 5 Raman spectrum in the range 1200–1700 cm^{-1}. Co-deposits: 77.1 SiC–6.4 TiC–16.5 C, $T_d = 1223$ K, first set of conditions.

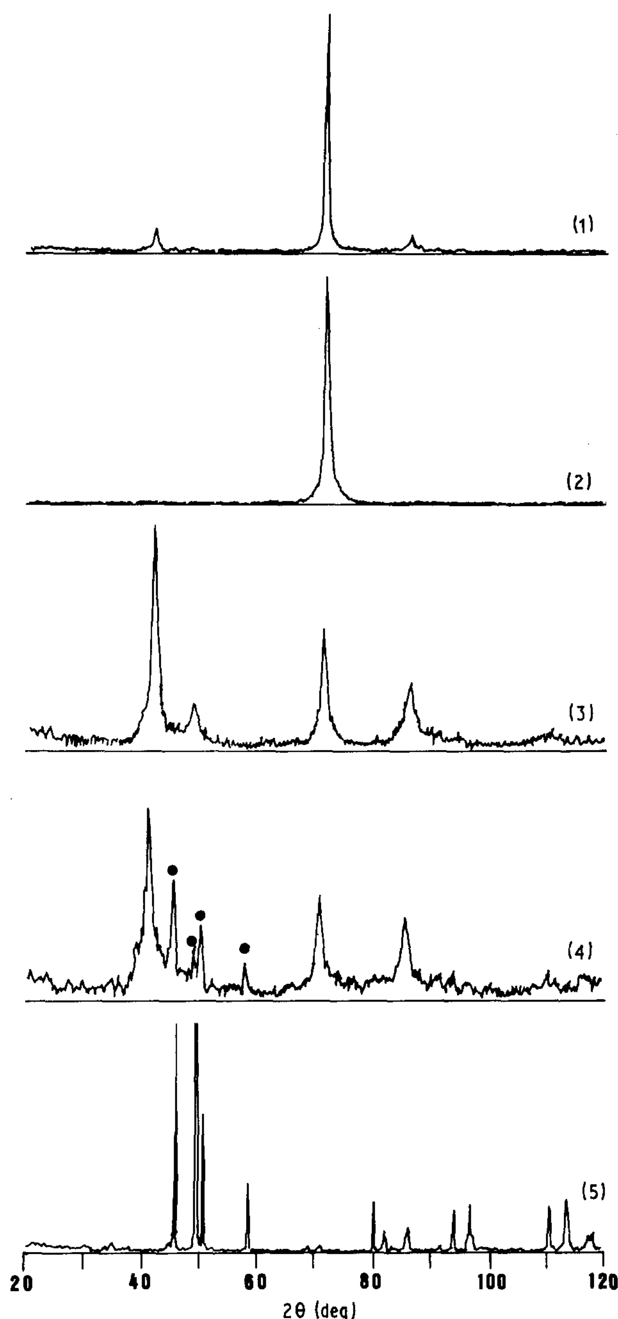

Figure 6 XRD patterns of (1) CVD SiC, $T_d = 1373$ K, (2) 80.8 SiC–11.5 TiC–7.7 C, $T_d = 1373$ K, (3) 94 SiC–6 TiC, $T_d = 1223$ K, (4) 91.7 SiC–8.3 $TiSi_2$, $T_d = 1123$ K, (5) CVD $TiSi_2$, $T_d = 1123$ K. (2–4) second set of conditions. (●) $TiSi_2$ X-ray diffraction lines.

same strong SiC (2 2 0) reflection found with a CVD SiC prepared at 1373 K (Fig. 6, Spectra 1 and 2). Therefore, with materials deposited at high temperature, the {1 1 0} planes were parallel to the substrate surface. With decreasing temperature, the (2 2 0) reflection became less apparent while the intensities of the (1 1 1), (2 0 0) and (3 1 1) reflections increased. Texture coefficients, TC($h k l$), as a function of deposition temperature, were calculated taking into account these four main reflections, from the following equation [15]

$$TC(hkl) = [I_m(hkl)/I_r(hkl)]/[0.25 \sum I_m \times (hkl)/I_r(hkl)] \quad (1)$$

were I_m is the measured intensity and I_r the intensity of the JCPDS powdered β-SiC. Fig. 7 shows that for

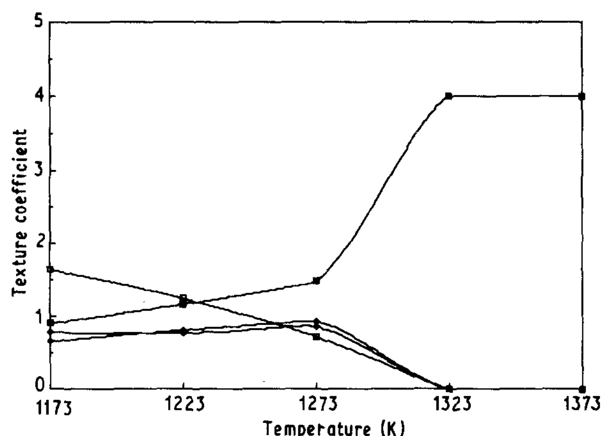

Figure 7 Texture coefficients of planes (□) (1 1 1), (◆) (2 0 0), (■) (2 2 0) and (◇) (3 1 1) as a function of the deposition temperature. Co-deposits prepared under the second set of deposition conditions: Table 1, Fig. 1b.

co-deposits prepared under the second set of deposition conditions (Table I), the ⟨2 2 0⟩ orientation occurs up to about 1323 K (TC(2 2 0) = 4), was drastically decreased below this, and a slightly preferred orientation ⟨1 1 1⟩ was observed at 1223 K. Moreover, TC($h k l$) values are similar at 1223 and 1173 K deposition temperatures, corresponding respectively, to the co-deposits 94 SiC–6 TiC and 92 SiC–8 $TiSi_2$ (mol %). Therefore, the texture of the grains in the co-deposits was probably governed by that of SiC crystallites, that is in agreement with the fact that SiC only or with dispersed TiC prepared at high temperature, showed the same remarkable ⟨2 2 0⟩ orientation (Fig. 6, Spectra 1 and 2). The effect of deposition temperature on the grain dimension was much less marked. In fact, the apparent crystallite size along the ⟨2 2 0⟩ direction estimated from the full width at half maximum of the corresponding diffraction peak using Scherrer's equation [16], decreased with temperature from about 15 nm to 10 nm.

4.3. Rate of deposition

Scanning electron micrographs of polished cross-sections of coated substrates, show that co-deposits for a 0.5 h experiment time have a regular contour (Fig. 8). In fact, only the thicker zone facing the reactants flow was considered to be representative of the deposition conditions. The thickness of this front zone, measured by optical microscopy, decreased with temperature from about 320 μm to 85 μm for the first set of deposition conditions and from about 385 μm to 60 μm in the second set. After having verified that the growth rates were almost independent of time (0.5–8 h), the deposition rate was expressed in thickness per hour and their logarithms were plotted versus reciprocal temperature. Arrhenius plots (Fig. 9) show linear relationships with breaks between low and high temperature slopes occurring at a temperature corresponding to a change in the dispersed phase: TiC above 1123 K and $TiSi_2$ below this. Moreover, the slope corresponding to the deposition of $TiSi_2$ is larger than that corresponding to TiC.

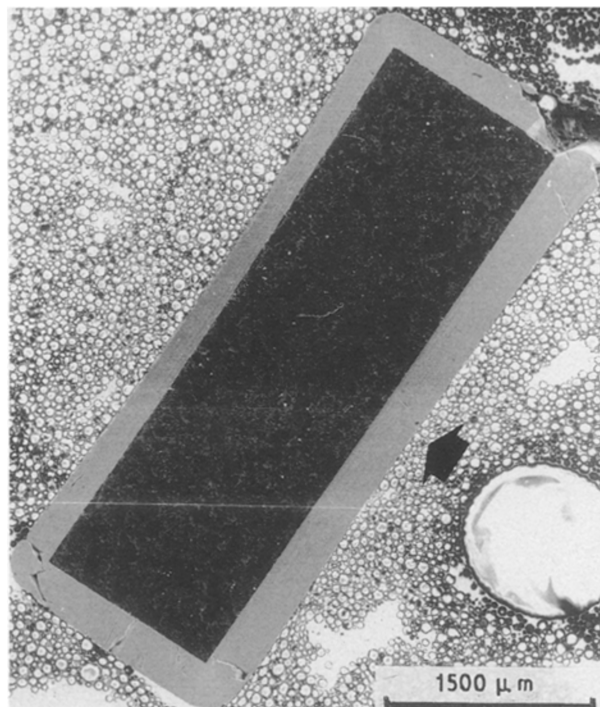

Figure 8 Scanning electron micrograph of a cross-section corresponding to a sample co-deposited at 1373 °C. The arrow indicates the thicker zone facing the reactants flow.

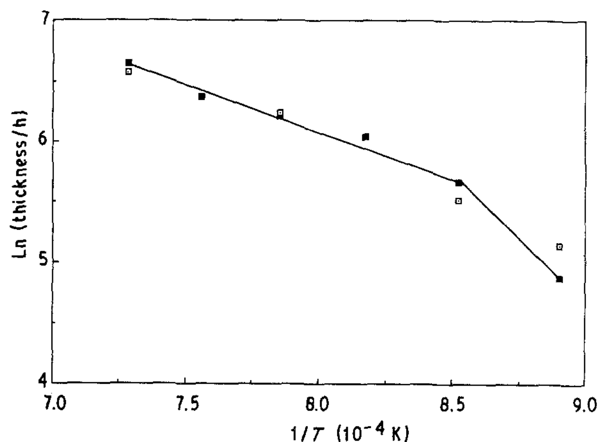

Figure 9 Arrhenius plots of the deposition rates under the (□) first and (■) second set of deposition conditions.

5. Conclusion

By co-deposition between 1373 and 1123 K, from the gas phase mixture $TiCl_4$, C_4H_{10}, SiH_2Cl_2 and H_2, homogeneous SiC–ceramic composites are available. The role of temperature has been well established. The nature of the dispersoid $TiSi_2$, TiC or TiC + C, strongly depends on the temperature. Furthermore, the higher the temperature, the stronger is the SiC ⟨2 2 0⟩ preferred orientation. In order to clarify the role of the gas phase composition, further experiments will be necessary to specify the dependence of the phase ratio in the deposited materials (and especially the presence or absence of free carbon) on this. Hardness measurements will be performed in order to show correlations between the mechanical behaviour of β-SiC–TiC (or $TiSi_2$) co-deposits and deposition conditions.

References

1. T. NARUSHIMA, T. GOTO and T. HIRAI, *J. Amer. Ceram. Soc.* **72** (1989) 1386.
2. S. MOTOJIMA and M. HAREGARWA, *J. Vac. Sci. Tech.* **A8** (1990) 3763.
3. T. M. BESMANN, D. P. STINTON and R. A. LOWDEN, *MRS Bull.* **13** (1988) 4550.
4. F. PORZ, G. GRATHWOHL and F. THUMMLER, *Mater. Sci. Engng* **71** (1985) 273.
5. P. REAGAN, W. COLE and F. HUFFMAN, *Ceram. Engng Sci. Proc.* **8** (1987) 958.
6. D. P. STINTON and W. J. LACKEY, *ibid.* **6** (1985) 707.
7. T. GOTO and T. HIRAI, in "Proceedings of the 10th International Conference on CVD", Honolulu, edited by G. W. Culler, (Electrochemical Society, 1987) pp. 1070–9.
8. M. TOUANEN, F. TEYSSANDIER, M. DUCARROIR and J. L. DEREP, *Mater. Sci. Engng A*, **147** (1991) 239
9. M. TOUANEN, Thesis, University of Perpignan, April 1990.
10. M. TOUANEN, F. TEYSSANDIER and M. DUCARROIR, *J. Mater. Sci. Lett.* **8** (1989) 98.
11. *Idem, J. Phys. Coll. C5* **50** (1989) 105.
12. M. KHELLAFI and B. LANG, *Rev. Phys. Appl.* **25** (1990) 329.
13. J. HEREMANS, I. RAHIM and M. S. DRESSLHAUS, *Phys. Rev. B* **32** (1985) 6742.
14. N. R. DANDO and M. A. TADAYYONI, *J. Amer. Ceram. Soc.* **73** (1990) 2242.
15. C. C. JIANG, T. GOTO and T. HIRAI, *J. Mater. Sci.* **25** (1990) 1086.
16. A. GUINIER, "Théore et Technique de la Radiocristallographie" (Dunod, Paris, 1964) pp. 462.

Received 14 October 1991
and accepted 29 January 1992